University of Wollongong

Research Online

Faculty of Science, Medicine and Health - Papers: part A

Faculty of Science, Medicine and Health

1-1-2015

Activation of the P2X7 receptor induces the rapid shedding of CD23 from human and murine B cells

Aleta Pupovac
University of Wollongong, ap251@uowmail.edu.au

Nicholas J. Geraghty
University of Wollongong

Debbie Watson
dwatson@uow.edu.au

Ronald Sluyter
University of Wollongong, rsluyter@uow.edu.au

Follow this and additional works at: https://ro.uow.edu.au/smhpapers

Part of the Medicine and Health Sciences Commons, and the Social and Behavioral Sciences Commons

Activation of the P2X7 receptor induces the rapid shedding of CD23 from human and murine B cells

Abstract

Activation of the P2X7 receptor by the extracellular damage-associated molecular pattern, adenosine 5'-triphosphate (ATP), induces the shedding of cell surface molecules including the low-affinity IgE receptor, CD23, from human leukocytes. A disintegrin and metalloprotease (ADAM) 10 mediates P2X7-induced shedding of CD23 from multiple myeloma RPMI 8226 B cells; however, whether this process occurs in primary B cells is unknown. The aim of the current study was to determine whether P2X7 activation induces the rapid shedding of CD23 from primary human and murine B cells. Flow cytometric and ELISA measurements showed that ATP treatment of human and murine B cells induced the rapid shedding of CD23. Treatment of cells with the specific P2X7 antagonist, AZ10606120, near-completely impaired ATP-induced CD23 shedding from both human and murine B cells. ATP-induced CD23 shedding was also impaired in B cells from P2X7 knockout mice. The absence of full-length, functional P2X7 in the P2X7 knockout mice was confirmed by immunoblotting of splenic cells, and by flow cytometric measurements of ATP-induced YO-PRO-12+ uptake into splenic B and T cells. The broad-spectrum metalloprotease antagonist, BB-94, and the ADAM10 antagonist, GI254023X, impaired P2X7-induced CD23 shedding from both human and murine B cells. These data indicate that P2X7 activation induces the rapid shedding of CD23 from primary human and murine B cells and that this process may be mediated by ADAM10.

Disciplines

Medicine and Health Sciences | Social and Behavioral Sciences

Activation of the P2X7 receptor induces the rapid shedding of CD23 from human and murine B cells

Aleta Pupovac[1,2], Nicholas J Geraghty[1,2], Debbie Watson[1,2] and Ronald Sluyter[1,2]

[1]School of Biological Sciences, University of Wollongong, Wollongong, NSW, Australia, [2]Illawarra Health and Medical Research Institute, Wollongong, NSW, Australia

Corresponding author:

Ronald Sluyter, School of Biological Sciences, University of Wollongong, Illawarra Health and Medical Research Institute, Wollongong, NSW 2522, Australia. Telephone: +61 2 4221 5508, Fax: +61 2 4221 8130, Email address: rsluyter@uow.edu.au (R. Sluyter)

Running title:

P2X7-induced CD23 shedding from B cells

Abstract

Activation of the P2X7 receptor by the extracellular damage-associated molecular pattern, adenosine 5'-triphosphate (ATP), induces the shedding of cell-surface molecules including the low-affinity IgE receptor, CD23, from human leukocytes. A disintegrin and metalloprotease (ADAM) 10 mediates P2X7-induced shedding of CD23 from multiple myeloma RPMI 8226 B cells, but whether this process occurs in primary B cells is unknown. The aim of the current study was to determine if P2X7 activation induces the rapid shedding of CD23 from primary human and murine B cells. Flow cytometric and ELISA measurements showed that ATP treatment of human and murine B cells induced the rapid shedding of CD23. Treatment of cells with the specific P2X7 antagonist, AZ10606120, near-completely impaired ATP-induced CD23 shedding from both human and murine B cells. ATP-induced CD23 shedding was also impaired in B cells from P2X7 knockout mice. The absence of full-length, functional P2X7 in the P2X7 knockout mice was confirmed by immunoblotting of splenic cells, and by flow cytometric measurements of ATP-induced YO-PRO-1^{2+} uptake into splenic B and T cells. The broad-spectrum metalloprotease antagonist, BB-94, and the ADAM10 antagonist, GI254023X, impaired P2X7-induced CD23 shedding from both human and murine B cells. This data indicates that P2X7 activation induces the rapid shedding of CD23 from primary human and murine B cells and that this process may be mediated by ADAM10.

Key words ADAM10; B lymphocyte; extracellular ATP; IgE receptor; purinergic receptor

CD23 is a 'low affinity', transmembrane receptor for IgE that is expressed on B cells and other leukocytes.[1] Transmembrane CD23 can be released from the cell-surface to form soluble CD23, which also binds IgE, and exerts cytokine-like activities on B cells and other leukocytes.[1] Soluble CD23 sustains growth of B cell precursors[2], promotes B and T cell differentiation,[3, 4] and drives cytokine release from monocytes[5]. The release of CD23 is mediated by membrane metalloproteases of the ADAM (a disintegrin and metalloprotease) family. ADAM10 is principally responsible for the constitutive and calcium-induced shedding of CD23.[6, 7]

Damage-associated molecular patterns (DAMPs) are essential in inflammation and immunity, and function as signals for cell stress, tissue injury and disease.[8] Extracellular adenosine 5'-triphosphate (ATP) is a well-characterised DAMP that activates the P2X7 receptor, a trimeric cation channel, which plays important roles in health and disease.[9] Activation of P2X7 by extracellular ATP causes the uptake of organic cations such as ethidium$^+$ and YO-PRO-1^{2+}.[10] P2X7 activation induces a number of downstream effects including the shedding of CD23 from human malignant B cells[11, 12] and human dendritic cells[13, 14]. Recently our group demonstrated that P2X7-induced CD23 shedding from the human multiple myeloma cell line, RPMI 8226, is mediated by ADAM10.[15] 2' (3')-O-(4-Benzoylbenzoyl) ATP (BzATP)-induced CD23 shedding from murine B cells is also mediated by ADAM10,[16, 17] but a direct role for P2X7 in this process was not established in these studies. Therefore, it remains unknown if P2X7 activation induces CD23 shedding from murine B cells, as well as from human B cells. The current study demonstrates that P2X7 activation induces the rapid shedding of CD23 from primary human and murine B cells and that this process possibly involves ADAM10.

Results

P2X7 activation induces rapid CD23 shedding from human B cells

ATP and BzATP at concentrations of 1 mM and 0.3 mM, respectively cause near-maximal activation of human P2X7.[18] Therefore, to first determine if ATP induces CD23 loss from human B cells, peripheral blood mononuclear cells (PBMCs) were incubated with 1 mM ATP for up to 30 min and cell-surface expression assessed by flow cytometry (Figure 1a). ATP induced a rapid loss of cell-surface CD23 from B cells with a $t_{1/2}$ of approximately 6 min (Figure 1b).

To determine whether ATP-induced CD23 loss was mediated by P2X7, PBMCs were incubated for 6 min (the $t_{1/2}$) in the absence or presence of 1 mM ATP, the most potent P2X7 agonist 0.3 mM BzATP, or the non-P2X7 agonists 1 mM adenosine diphosphate (ADP) and uridine 5'-triphosphate (UTP). ATP and BzATP induced a 49 ± 9% and 60 ± 9% loss of cell-surface CD23, respectively, while ADP and UTP had no effect on CD23 expression compared to cells incubated without nucleotide (Figure 1c).

The P2X7 antagonist AZ10606120,[19] at a concentration of 100 nM results in near-complete inhibition of human P2X7.[20] Therefore, to confirm that ATP-induced loss of CD23 was mediated by P2X7, PBMCs were pre-incubated in the absence or presence of 100 nM AZ10606120, and 1 mM ATP-induced CD23 loss determined by flow cytometry. AZ10606120 impaired ATP-induced CD23 loss by 89 ± 12% (Figure 1d). In the absence of ATP, AZ10606120 did not alter CD23 expression (Figure 1d).

To determine if the P2X7-induced loss of cell-surface CD23 was due to CD23 shedding, PBMCs were incubated in the absence or presence of 1 mM ATP for 20 min, and the relative amount of soluble CD23 in cell-free supernatants quantified by ELISA. Incubation of cells with ATP resulted in a significantly higher release of soluble CD23 compared with cells incubated in the absence of ATP (Figure 1e).

Murine B cells express functional P2X7

The presence of functional P2X7 on primary human B cells is well-established,[21] but less well known for murine B cells. Similar to human P2X7, ATP and BzATP at concentrations of 1 mM and 0.3 mM, respectively result in near-maximal activation of murine P2X7.[18] While the P2X7 antagonist AZ10606120, at a concentration of 10 μM results in near-complete inhibition of murine P2X7.[22] Therefore, to first test whether functional P2X7 was present on murine B cells from C57BL/6 and DBA/1 mice, splenic cells from these two strains were pre-incubated in the absence or presence of 10 μM AZ10606120, and 1 mM ATP-induced YO-PRO-1^{2+} uptake into B cells determined by flow cytometry. C57BL/6 mice were studied because of the availability of the Pfizer P2X7 knockout mice,[23] which had been backcrossed onto a C57BL/6 background.[24] DBA/1 mice were also studied as this strain has been used to demonstrate a role for CD23 in rheumatoid arthritis[25], a disease in which P2X7 is also thought to be involved.[26, 27] ATP-induced significant YO-PRO-1^{2+} uptake into murine B cells, from either C57BL/6 or DBA/1 mice, compared to YO-PRO-1^{2+} uptake in the absence of ATP (Figure 2a, b). Moreover, 10 μM AZ10606120 significantly impaired ATP-induced YO-PRO-1^{2+} uptake in B cells from C57BL/6 or DBA/1 mice, by $88 \pm 14\%$ or $95 \pm 8\%$, respectively (Figure 2a, b). In the absence of ATP, AZ10606120 did not alter YO-PRO-1^{2+} uptake in B cells from either mouse strain (Figure 2a, b).

P2X7 activation induces rapid CD23 shedding from murine B cells

To determine if ATP induces CD23 loss from murine B cells, splenic cells were incubated with 1 mM ATP for up to 30 min and cell-surface CD23 expression assessed by flow cytometry (Figure 3a, b). ATP induced a rapid loss of cell-surface CD23 from B cells from both C57BL/6 and DBA/1 mice with a $t_{1/2}$ of approximately 7 min (Figure 3c).

To determine if ATP-induced CD23 loss was mediated by P2X7, cells from both mouse strains were incubated for 7 min (the $t_{1/2}$) in the absence or presence of 1 mM ATP, 0.3 mM BzATP, 1 mM ADP or 1 mM UTP. Similar to above (Figure 3c), ATP induced a 37 ± 4% and 57 ± 4% loss of cell-surface CD23 in B cells from C57BL/6 and DBA/1 mice, respectively (Figure 3d, e). BzATP induced a 33 ± 8% and 58 ± 5% loss of cell-surface CD23 in B cells from C57BL/6 and DBA/1 mice, respectively, while ADP and UTP had no effect compared to cells incubated without nucleotide in either mouse strain (Figure 3d, e).

To confirm that ATP-induced loss of CD23 was mediated by P2X7, cells were pre-incubated in the absence or presence of 10 μM AZ10606120, and 1 mM ATP-induced CD23 loss determined by flow cytometry. AZ10606120 impaired ATP-induced CD23 loss by 95 ± 8% and 97 ± 6% in B cells from C57BL/6 and DBA/1 mice respectively (Figure 3f, g). In the absence of ATP, AZ10606120 did not alter CD23 expression in B cells from either mouse strain (Figure 3f, g).

Finally, to further confirm a role for P2X7 in ATP-induced CD23 loss, P2X7 knockout mice were used. Flow cytometric measurements demonstrated that the amount of CD23 expression between control-treated B cells from wild-type and P2X7 knockout mice was similar (Figure 3h). In contrast, incubation with 1 mM ATP

induced a loss of cell-surface CD23 in B cells from wild-type mice (34 ± 10% loss) but ATP-induced CD23 loss from B cells from P2X7 knockout mice was minimal (8 ± 7% loss) (Figure 3h).

To indirectly assess if the ATP-induced loss of CD23 from murine B cells was a result of CD23 shedding or internalisation, splenic cells from C57BL/6 mice were incubated in the absence or presence of 1 mM ATP for 20 min and the expression of cell-surface CD23 on fixed cells, or total CD23 in fixed and permeabilised cells was examined by flow cytometry. CD23 expression was similar in fixed cells compared to fixed and permeabilised cells (Figure 4a) suggesting that the P2X7-induced loss of CD23 was due to CD23 shedding rather than internalisation.

To directly determine if the P2X7-induced loss of cell-surface CD23 was due to CD23 shedding, splenic cells from C57BL/6 wild-type and P2X7 knockout mice were incubated in the absence or presence of 1 mM ATP for 20 min, and the relative amount of soluble CD23 in cell-free supernatants quantified by ELISA. Incubation of wild-type cells with ATP resulted in a significantly higher release of soluble CD23 compared with P2X7 knockout cells incubated with ATP, or cells of either strain incubated in the absence of ATP (Figure 4b). Moreover, the amount of soluble CD23 release from P2X7 knockout cells incubated in the absence or presence of ATP was similar to that of wild-type cells incubated in the absence of ATP (Figure 4b).

Splenic cells from P2X7 knockout mice do not express full-length, functional P2X7

Recent evidence indicates that Pfizer P2X7 knockout mice,[23] from which the P2X7 knockout mice in the current study were derived,[24] express three novel C-terminal truncated P2X7 variants termed 13A (~60 kDa), 13B (~60 kDa) and hybrid (~70 kDa)

P2X7.[28] Pfizer P2X7 knockout mice were generated by targeting exon 13 of the *P2RX7* gene,[23] and PCR with primers to exons 9 and 11 of the *P2RX7* gene demonstrates P2X7 expression in various tissues from these mice.[28] Consistent with these findings, quantitative RT-PCR with primers to exons 1 and 2 of the *P2RX7* gene revealed significant expression of *P2RX7* transcripts in the splenic cells from both wild-type and P2X7 knockout mice (Figure 5a). Relative P2X7 expression was 2-fold higher in P2X7 knockout splenic cells compared to wild-type splenic cells but this failed to reach statistical significance (Figure 5a). This data indicates the potential presence of escape variants of P2X7 in the P2X7 knockout mice used to study ATP-induced CD23 shedding above.

To determine if the mRNA transcripts for P2X7 detected above (Figure 5a) were translated into protein, splenic cells of these mice were examined by immunoblotting with an antibody against the extracellular domain of murine P2X7, which can detect full-length P2X7, as well as the C-terminal truncated P2X7 variants.[28] Murine RAW 264.7 macrophages, which are known to express full-length P2X7,[29] were included as a positive control. Immunoblotting identified a major band at 81 kDa, corresponding to glycosylated full-length P2X7, in wild-type splenic cells and RAW 264.7 macrophages, but not in P2X7 knockout splenic cells (Figure 5b). Immunoblotting also revealed a major band at 75 kDa in all three cell types (Figure 5b). The size of this band corresponds to that of the hybrid C-terminal truncated P2X7 variant present in Pfizer P2X7 knockout mice. However, this variant contains a short sequence of the targeting vector originally used to disrupt the *P2RX7* gene,[28] thus this variant cannot be present in wild-type splenic cells or RAW 264.7 macrophages. Therefore, this 75 kDa band most likely represents non-specific binding. Immunoblotting also detected a major band at 154 kDa in wild-type and P2X7 knockout splenic cells, but not in

RAW264.7 macrophages (Figure 5b). This band does not correspond to any known P2X7 variant and thus most likely represents non-specific binding.

Flow cytometric measurements of ATP-induced YO-PRO-1^{2+} uptake were then used to confirm the absence of functional P2X7 in splenic B cells from the P2X7 knockout mice used to study ATP-induced CD23 shedding above. T cells from GlaxoSmithKline P2X7 knockout mice, derived by targeting exon 1 of the *P2RX7* gene,[30] express P2X7k, an alternate splice variant that has escaped gene inactivation and encodes functional receptors.[31-33] Therefore, ATP-induced YO-PRO-1^{2+} uptake into splenic T cells was also assessed. As expected, 1 mM ATP induced YO-PRO-1^{2+} uptake into both B and T cells from wild-type mice (Figure 5c). In contrast, 1 mM ATP failed to induce YO-PRO-1^{2+} uptake into either B or T cells from P2X7 knockout mice (Figure 5c). Collectively, these results indicate that the P2X7 knockout mice used to study ATP-induced CD23 shedding above do not express full-length, functional P2X7.

ADAM10 mediates P2X7-induced CD23 shedding from human and murine B cells

To determine a role for metalloproteases in P2X7-induced CD23 shedding, human PBMCs or murine splenic cells were pre-incubated in the absence or presence of the broad-spectrum metalloprotease antagonist, BB-94,[34] or the ADAM10 antagonist, GI254023X,[35] and 1 mM ATP-induced CD23 shedding from B cells determined by flow cytometry. BB-94 (1 μM) impaired P2X7-induced CD23 shedding from B cells by 66 ± 10%, 100 ± 0% and 96 ± 6% from human, C57BL/6 and DBA/1 mice, respectively (Figure 6a-c). GI254023X (3 μM) impaired P2X7-induced CD23 shedding from B cells by 77 ± 20%, 83 ± 29% and 100 ± 0% from human, C57BL/6

and DBA/1 mice respectively (Figure 6d-f). In the absence of ATP, BB-94 did not alter basal CD23 expression in human and murine cells (Figure 6a-c). Likewise, GI254023X did not alter basal CD23 expression in human or DBA/1 B cells (Figure 6d, f). In contrast, GI254023X significantly reduced basal (constitutive) CD23 shedding from C57BL/6 B cells (Figure 6e).

Discussion

The current study, shows for the first time that P2X7 activation induces the rapid shedding of CD23 from primary human and murine B cells. This was confirmed by a series of experiments. First, ATP induced the rapid cell-surface loss of CD23 shedding with a $t_{1/2}$ of approximately 6 and 7 min from human and murine B cells, respectively. Second, the most potent P2X7 agonist BzATP also induced the rapid cell-surface loss of CD23, whereas the non-agonists ADP and UTP had no effect. Third, a specific P2X7 antagonist, AZ10606120,[19] almost completely impaired ATP-induced CD23 shedding in both human and murine B cells. Fourth, ATP failed to induce CD23 shedding from B cells from C57BL/6 P2X7 knockout mice. Finally, measurements of soluble CD23 (as well as total CD23 expression for murine B cells) indicated that cell-surface loss of CD23 was due to shedding from both human and murine B cells.

Using the ADAM10 inhibitor, GI254023X,[35] the current study also shows that P2X7-induced CD23 shedding from human and murine B cells is possibly mediated, at least in part, by ADAM10. This finding is consistent with a role for ADAM10 in P2X7-

induced CD23 shedding from human RPMI 8226 myeloma cells.[15] Remarkably, the rate of P2X7-induced CD23 shedding from human and murine B cells was similar to that observed for RPMI 8226 cells ($t_{1/2}$ of ~7 min) indirectly supporting the involvement of a common mechanism. A potential role for ADAM10 in P2X7-induced CD23 shedding from primary B cells is indirectly supported by other studies. ATP-induced CD23 shedding from human leukaemic monocytic U937 cells[7], and BzATP-induced CD23 shedding from Chinese hamster ovary cells[16] and murine B cells[17], are also mediated by ADAM10. The possibility remains that other metalloproteases may also be involved in P2X7-induced CD23 shedding from human and murine B cells. ADAM 8, 15, 28 and 33 have been associated with constitutive CD23 shedding from CD23-transfected HEK293 cells[36] and primary murine embryonic fibroblasts[6], although ADAM10 was identified as the principal sheddase of CD23.[6]

It remains unknown how P2X7 potentially activates ADAM10. Repeated attempts using a Fluorogenic Peptide Substrate III assay (R&D Systems, Minneapolis, MN) (which detects the activity of ADAM10, as well as ADAM8, 9 and 17) were unable to demonstrate that ATP could stimulate ADAM10 activation on RPMI 8226 cells despite detectable ADAM activity on these cells in the absence of ATP (Pupovac and Sluyter, unpublished observations). Thus, the possibility remains that P2X7 activation induces cell-surface CD23 shedding through the co-localisation of ADAM10 and CD23, rather than by directly stimulating ADAM10 activity. Finally, using a candidate approach, our previous studies also failed to identify potential intracellular signalling molecules involved in P2X7-induced CD23 shedding.[20]

The current study demonstrates the presence of functional P2X7 on murine B cells from both C57BL/6 and DBA/1 mice. Although the presence of functional P2X7 on

human B cells is well established, reports of functional P2X7 on murine B cells are limited. In the current study, P2X7 activation induced CD23 shedding from murine B cells. Moreover, ATP was shown to induce YO-PRO-1^{2+} uptake into murine B cells, and that the process was impaired by AZ10606120 and in B cells from P2X7 knockout mice. Of note, the relative amounts of P2X7-mediated YO-PRO-1^{2+} uptake and rates of P2X7-mediated CD23 shedding were similar between C57BL/6 and DBA/1 mice. This similar amount of relative P2X7 function most likely reflects the presence of the partial loss-of-function mutation P451L in both of these strains.[37]

A previous study has shown that LPS can induce CD23 shedding from human and murine B cells, and that this process is mediated by Toll-like receptor 4 (TLR4) and matrix metalloprotease 9.[38] However it remains unlikely that LPS, potentially present in the reagents used, was responsible for the ATP-induced CD23 observed in the current study. First, ATP induced the rapid (<30 min) shedding of CD23; in contrast LPS induces the slow (24 h) shedding of CD23.[38] Second, ADP and UTP failed to induce CD23 shedding, while ATP-induced shedding was impaired by P2X7 antagonists and in B cells from P2X7 knockout mice. Nevertheless, future studies using B cells from either C3H/HeJ mice, which are hyporesponsive to LPS due to single point mutation in the *TLR4* gene,[39] or TLR4 knockout mice will be of value to address this potential issue further.

Human genetic[27, 40] and murine model studies[26, 41] suggest a role for P2X7 in rheumatoid arthritis and Sjogren's syndrome. The role of P2X7 in these disorders has largely been attributed to the release of the proinflammatory cytokines, interleukin-1β and interleukin-18.[26, 42] However, synovial or circulating soluble CD23 is elevated in patients with rheumatoid arthritis[43, 44] or Sjogren's syndrome[45]. Moreover, B cells also play major roles in the pathogenesis of these disorders through the production of

autoantibodies.[46, 47] Thus, the possibility remains that P2X7-induced shedding of pro-inflammatory soluble CD23 from B cells may also be involved in rheumatoid arthritis, Sjogren's syndrome or other disorders. However, evidence directly linking B cells, P2X7 and CD23 in inflammatory and autoimmune disease is lacking. An alternate, but not mutually exclusive possibility is that ATP-induced CD23 shedding is an early event of P2X7-mediated apoptosis. In the current study, 30 min incubation with ATP caused a small but significant amount of apoptosis, determined by forward scatter (cell shrinkage) and 7AAD uptake (loss of membrane integrity),[48] in murine but not human B cells compared to respective B cells incubated in the absence of ATP (results not shown). In contrast, human and murine B cell apoptosis was not increased following 6-7 min treatment with either ATP or BzATP compared to control treatment, nor was B cell apoptosis increased following incubation with AZ10606120 in the absence or presence of ATP (results not shown). Nevertheless given that P2X7 activation can induce apoptosis in human PBMCs[49] and murine splenic cells,[50] the possibility remains that ATP-induced CD23 shedding is an early upstream event in P2X7-mediated apoptosis of B cells.

In conclusion, this study demonstrates human and murine P2X7 activation induces the rapid shedding of CD23 from B cells. Moreover, the study indicates a potential role for ADAM10 in this process.

Methods

Reagents

Ficoll Paque^{TM} PLUS was from GE Healthcare Bio-Sciences (Uppsala, Sweden). DMEM/F12 medium, YO-PRO-1 iodide, TRIzol reagent, and TaqMan Universal Master Mix II with uracil-DNA glycosylase (UDG) and Gene Expression Assays were from Life Technologies (Grand Island, NY). Red blood cell lysis buffer, ATP, BzATP, ADP, UTP, paraformaldehyde and RNA*later* were from Sigma-Aldrich (St. Louis, MO). Dimethyl sulphoxide (DMSO) and Tween-20 were from Amresco (Solon, OH). AZ10606120 and BB-94 (Batimastat) were from Tocris Bioscience (Ellisville, MO). GI254023X was kindly provided by GlaxoSmithKline (Stevenage, United Kingdom). 7-Aminoactinomycin D (7AAD) was from Enzo Life Sciences (Plymouth Meeting, PA). Phycoerythrin (PE)-conjugated murine anti-human CD23 (clone EBVCS2), PE-conjugated isotype control (clone P3.6.2.8.1), fluorescein isothiocyanate (FITC)-conjugated rat anti-murine CD23 (clone B3B4), FITC-conjugated isotype control (clone eBR2a), allophycocyanin (APC)-conjugated murine anti-human CD19 (clone HIB19) and APC-conjugated rat anti-murine CD19 (clone eBio1D3) monoclonal antibodies (mAb) were from eBioscience (San Diego, CA). Peridinin chlorophyll protein/cyanine 5.5 (PerCP/Cy5.5)-conjugated hamster anti-murine CD3 (clone 145-2C11) mAb was from BioLegend (San Diego, CA). Rabbit anti-murine P2X7 polyclonal antibody (extracellular domain) was from Alomone Labs (Jerusalem, Israel).

Cells

All experiments involving humans and mice were approved by the University of Wollongong ethics committee. Human peripheral blood was collected into VACUETTE® lithium heparin tubes (Greiner Bio-One, Frickenhausen, Germany) and diluted with an equal volume of phosphate buffered saline (PBS). PBMCs were separated by density gradient centrifugation over Ficoll-Paque™ PLUS (560 x g for 30 min), washed once in PBS (450 x g for 10 min) and then twice in NaCl medium (145 mM NaCl, 5 mM KCl, 5 mM glucose, 10 mM HEPES, pH 7.4). The mean percentage of CD19$^+$ cells within the 13 PBMC preparations used was 4.0% (range 2.5-7.5%). C57BL/6 and DBA/1 mice were from Animal Resources Centre (Perth, Australia) or Australian BioResources (Moss Vale, Australia). P2X7 knockout mice[23] backcrossed onto a C57BL/6 background, were bred at the Centenary Institute (Sydney, Australia) or the University of Wollongong (Wollongong, Australia).[24] Mice were euthanised and spleens collected in ice-cold PBS. Spleens were teased apart using a needle and forceps in ice-cold PBS, and cells were filtered through a 70 µm nylon cell strainer (BD, San Jose, CA). Splenic cells were then washed in ice-cold PBS (400 x g for 5 min) and the pellet resuspended in red blood cell lysis buffer. Red blood cells were lysed for 3 min at room temperature with agitation and the remaining leukocytes were washed once with ice-cold DMEM/F12 medium. Cells were then washed twice in NaCl medium (for functional assays) or PBS (for PCR or immunoblotting). Murine RAW 264.7 macrophages (American Type Culture Collection, Manassas, VA) were maintained as described.[24]

Measurement of nucleotide-induced CD23 shedding by flow cytometry

Nucleotide-induced CD23 shedding from cells was indirectly assessed by flow cytometric measurements of ATP-induced loss of cell-surface CD23 as described.[11] Briefly, PBMCs or splenic cells suspended in NaCl medium (1 x 10^6 cells/ml), were incubated in the absence or presence of nucleotide (as indicated) for up to 30 min at 37ºC. In some experiments, cells in NaCl medium were pre-incubated at 37°C for 15 min in the absence or presence of antagonist, and then in the absence or presence of 1 mM ATP (as indicated). Incubations with nucleotide were stopped by addition of an equal volume of ice-cold $MgCl_2$ medium (NaCl medium containing 20 mM $MgCl_2$) and centrifugation. Cells were then washed once with NaCl medium and incubated with species-specific fluorochrome-conjugated anti-CD23 or isotype control mAb, anti-CD19 mAb and 7AAD for 30 min at 4ºC. The mean fluorescence intensity (MFI) of cell-surface CD23 expression on viable $CD19^+7AAD^-$ cells was determined using a BD LSR II flow cytometer (using band-pass filters 575/26 or 515/20 nm for CD23, 660/20 nm for CD19 and 695/40 nm for 7AAD) and FlowJo software (Tree Star, Ashland, OR).

Cell-surface and total CD23 expression following treatment was compared as previously described.[51] Splenic cells were washed once with NaCl medium and labelled with APC-conjugated anti-murine CD19 and 7AAD for 30 min at 4ºC. Cells were fixed by suspension in ice-cold 0.25% paraformaldehyde in PBS for 1 hour at 4°C. Cells were then either washed once in cold PBS (fixed) or in 0.2% Tween-20 in PBS (fixed and permeabilised) and labelled with FITC-conjugated anti-murine CD23 or isotype control mAb for 30 min at 4°C. The MFI of cell-surface and total (cell-surface and intracellular) CD23 expression on $CD19^+$ cells was determined using flow

cytometry (using band-pass filters 515/20 nm for CD23, 660/20 nm for CD19 and 695/40 nm for 7AAD) and FlowJo software.

Measurement of soluble CD23 by ELISA

PBMCs or splenic cells suspended in NaCl medium (5 x 10^6 cells/ml), were incubated in the absence or presence of 1 mM ATP for 20 min at 37°C. Incubations were stopped by centrifugation (11000 x g for 10 s). Cell-free supernatants were stored at -80°C until required. Soluble CD23 was quantified using the Human CD23/Fcε RII Quantikine ELISA Kit or the Mouse CD23/Fcε RII DuoSet ELISA Development Kit (both R&D Systems), according to the manufacturer's instructions.

Measurement of P2X7 pore formation by flow cytometry

P2X7-induced pore formation in murine B cells was assessed by flow cytometric measurements of ATP-induced YO-PRO-1^{2+} uptake as described.[52] Briefly, splenic cells suspended in NaCl medium (1 x 10^6 cells/ml) were pre-incubated in the absence or presence of 10 µM AZ10606120 (as indicated), and then with 1 µM YO-PRO-1^{2+} in the absence or presence of ATP (as indicated) for 15 min at 37°C. Incubations were stopped by addition of an equal volume of ice-cold $MgCl_2$ medium and centrifugation. Cells were washed once with NaCl medium. Cells were labelled with APC-conjugated anti-murine CD19 mAb (and in some experiments, also with PerCP/Cy5.5-conjugated anti-murine CD3 mAb) and washed once with NaCl medium. The MFI of YO-PRO-1^{2+} uptake into $CD19^+$ cells (or in some experiments, $CD19^+CD3^-$ or $CD19^-CD3^+$ cells) was determined using flow cytometry (using band-pass filters 515/20 nm for YO-PRO-1^{2+}, 695/40 nm for CD3 and 660/20 nm for CD19) and FlowJo software.

Measurement of P2X7 by quantitative real time-PCR

Mouse spleens were stored in RNA*later* at -20°C until required. Total RNA was isolated using TRIzol reagent according to the manufacturer's instructions. cDNA synthesis was performed using a qScript cDNA Synthesis Kit (Quanta Biosciences, Gaithersburg, MD) following the manufacturer's instructions. Real-time PCR reactions consisted of 5 μL 2X TaqMan Universal Master Mix II with UDG, 0.5 μL of 20X TaqMan Gene Expression Assay (specific primers/probes), 2 μL cDNA and sterile water in a total volume of 10 μL. Each PCR reaction was performed in triplicate. Quantitative real-time PCR was performed using standard primers for murine *P2RX7* (FAM-labelled; Mm00440578_m1) and murine *GAPDH* (VIC-labelled; Mm99999915_g1). Real-time PCR was performed on an Eco Real-time PCR System (Illumina, San Diego, CA) in sealed 48-well plates (Gene Target Solutions, Dural, Australia). The PCR cycle consisted of an initial UDG incubation step of 50°C for 2 min, polymerase activation step of 95°C for 10 min and 40 cycles of 95°C for 15 s and 60°C for 1 min. Relative gene expression was normalised to the murine *GAPDH* housekeeping gene and determined using Eco Software v5.0 (Illumina).

Measurement of P2X7 by immunoblotting

Immunoblotting of murine cells was performed as described.[53] Briefly, whole cell lysates were separated under reducing conditions using Any kD Mini-PROTEAN TGX Stain-Free Gels (Bio-Rad, Hercules, CA) and transferred to nitrocellulose membrane (Bio-Rad), and immunoblotting was performed using an anti-P2X7 antibody. To confirm equal protein loading between splenic cell samples within stain-free gels, total protein was assessed using a Bio-Rad Criterion Stain Free Imager (results not shown).

Presentation of data and statistics

Data is presented as mean ± SD from individual people or mice except where stated. Differences between groups were compared using an unpaired Student's t-test for single comparisons or one-way ANOVA (using Tukey's multiple comparison test) except for human ELISA data, for which a paired Student's t-test was used. Statistical comparisons were performed using Prism 5 (Windows version 5.01; GraphPad Software, San Diego, CA) with $P < 0.05$ considered significant.

Acknowledgements

References

1.   Acharya M, Borland G, Edkins AL, Maclellan LM, Matheson J, Ozanne BW *et al.* CD23/FcεRII: molecular multi-tasking. *Clin Exp Immunol* 2010; **162:** 12-23.

2.   Borland G, Edkins AL, Acharya M, Matheson J, White LJ, Allen JM *et al.* αvβ5 integrin sustains growth of human pre-B cells through an RGD-independent interaction with a basic domain of the CD23 protein. *J Biol Chem* 2007; **282:** 27315-26.

3.   Liu YJ, Cairns JA, Holder MJ, Abbot SD, Jansen KU, Bonnefoy JY *et al.* Recombinant 25-kDa CD23 and interleukin 1α promote the survival of germinal center B cells: evidence for bifurcation in the development of centrocytes rescued from apoptosis. *Eur J Immunol* 1991; **21:** 1107-14.

4.   Mossalayi MD, Lecron JC, Dalloul AH, Sarfati M, Bertho JM, Hofstetter H *et al.* Soluble CD23 (FcεRII) and interleukin 1 synergistically induce early human thymocyte maturation. *J Exp Med* 1990; **171:** 959-64.

5.   Hermann P, Armant M, Brown E, Rubio M, Ishihara H, Ulrich D *et al.* The vitronectin receptor and its associated CD47 molecule mediates proinflammatory cytokine synthesis in human monocytes by interaction with soluble CD23. *J Cell Biol* 1999; **144:** 767-75.

6.   Weskamp G, Ford JW, Sturgill J, Martin S, Docherty AJ, Swendeman S *et al.*
        ADAM10 is a principal 'sheddase' of the low-affinity immunoglobulin E
        receptor CD23. *Nat Immunol* 2006; **7:** 1293-8.

7.   Lemieux GA, Blumenkron F, Yeung N, Zhou P, Williams J, Grammer AC *et
        al.* The low affinity IgE receptor (CD23) is cleaved by the metalloproteinase
        ADAM10. *J Biol Chem* 2007; **282:** 14836-44.

8.   Chen GY, Nunez G. Sterile inflammation: sensing and reacting to damage.
        Nat Rev Immunol 2010; **10:** 826-37.

9.   Bartlett R, Stokes L, Sluyter R. The P2X7 receptor channel: recent
        developments and the use of P2X7 antagonists in models of disease.
        Pharmacol Rev 2014; **66:** 1-38.

10.   Cankurtaran-Sayar S, Sayar K, Ugur M. P2X7 receptor activates multiple
        selective dye-permeation pathways in RAW 264.7 and human embryonic
        kidney 293 cells. *Mol Pharmacol* 2009; **76:** 1323-32.

11.   Farrell AW, Gadeock S, Pupovac A, Wang B, Jalilian I, Ranson M *et al.* P2X7
        receptor activation induces cell death and CD23 shedding in human RPMI
        8226 multiple myeloma cells. *Biochim Biophys Acta* 2010; **1800:** 1173-82.

12.   Gu B, Bendall LJ, Wiley JS. Adenosine triphosphate-induced shedding of
       CD23 and L-selectin (CD62L) from lymphocytes is mediated by the same
       receptor but different metalloproteases. *Blood* 1998; **92:** 946-51.

13.   Sluyter R, Wiley JS. Extracellular adenosine 5'-triphosphate induces a loss of
       CD23 from human dendritic cells via activation of P2X7 receptors. *Int
       Immunol* 2002; **14:** 1415-21.

14.   Georgiou JG, Skarratt KK, Fuller SJ, Martin CJ, Christopherson RI, Wiley JS
       et al. Human epidermal and monocyte-derived langerhans cells express
       functional P2X receptors. *J Invest Dermatol* 2005; **125:** 482-90.

15.   Pupovac A, Foster CM, Sluyter R. Human P2X7 receptor activation induces
       the rapid shedding of CXCL16. *Biochem Biophys Res Commun* 2013; **432:**
       626-31.

16.   Le Gall SM, Bobe P, Reiss K, Horiuchi K, Niu XD, Lundell D *et al.* ADAMs
       10 and 17 represent differentially regulated components of a general shedding
       machinery for membrane proteins such as transforming growth factor α, L-
       selectin, and tumor necrosis factor α. *Mol Biol Cell* 2009; **20:** 1785-94.

17.   Le Gall SM, Maretzky T, Issuree PD, Niu XD, Reiss K, Saftig P *et al.* ADAM17 is regulated by a rapid and reversible mechanism that controls access to its catalytic site. *J Cell Sci* 2010; **123:** 3913-22.

18.   Donnelly-Roberts DL, Namovic MT, Han P, Jarvis MF. Mammalian P2X7 receptor pharmacology: Comparison of recombinant mouse, rat and human P2X7 receptors. *Br J Pharmacol* 2009; **157:** 1203-1214.

19.   Michel AD, Chambers LJ, Walter DS. Negative and positive allosteric modulators of the P2X$_7$ receptor. *Br J Pharmacol* 2008; **153:** 737-50.

20.   Pupovac A, Stokes L, Sluyter R. CAY10593 inhibits the human P2X7 receptor independently of phospholipase D1 stimulation. *Purinergic Signal* 2013; **9:** 609-19.

21.   Gu BJ, Zhang WY, Bendall LJ, Chessell IP, Buell GN, Wiley JS. Expression of P2X$_7$ purinoceptors on human lymphocytes and monocytes: evidence for nonfunctional P2X$_7$ receptors. *Am J Physiol Cell Physiol* 2000; **279:** C1189-97.

22.   Bartlett R, Yerbury JJ, Sluyter R. P2X7 Receptor activation induces reactive oxygen species formation and cell death in murine EOC13 microglia. *Mediators Inflamm* 2013; **2013:** 271813.

23.   Solle M, Labasi J, Perregaux DG, Stam E, Petrushova N, Koller BH *et al.* Altered cytokine production in mice lacking P2X$_7$ receptors. *J Biol Chem* 2001; **276:** 125-32.

24.   Tran JN, Pupovac A, Taylor RM, Wiley JS, Byrne SN, Sluyter R. Murine epidermal Langerhans cells and keratinocytes express functional P2X7 receptors. *Exp Dermatol* 2010; **19:** e151-7.

25.   Plater-Zyberk C, Bonnefoy JY. Marked amelioration of established collagen-induced arthritis by treatment with antibodies to CD23 in vivo. *Nat Med* 1995; **1:** 781-5.

26.   Labasi JM, Petrushova N, Donovan C, McCurdy S, Lira P, Payette MM *et al.* Absence of the P2X7 receptor alters leukocyte function and attenuates an inflammatory response. *J Immunol* 2002; **168:** 6436-45.

27.   Portales-Cervantes L, Nino-Moreno P, Salgado-Bustamante M, Garcia-Hernandez MH, Baranda-Candido L, Reynaga-Hernandez E *et al.* The His155Tyr (489C>T) single nucleotide polymorphism of P2RX7 gene confers an enhanced function of P2X7 receptor in immune cells from patients with rheumatoid arthritis. *Cell Immunol* 2012; **276:** 168-75.

28.   Masin M, Young C, Lim K, Barnes SJ, Xu XJ, Marschall V *et al.* Expression, assembly and function of novel C-terminal truncated variants of the mouse P2X7 receptor: Re-evaluation of P2X7 knockouts. *Br J Pharmacol* 2012; **165:** 978-993.

29.   Constantinescu P, Wang B, Kovacevic K, Jalilian I, Bosman GJ, Wiley JS *et al.* P2X7 receptor activation induces cell death and microparticle release in murine erythroleukemia cells. *Biochim Biophys Acta* 2010; **1798:** 1797-1804.

30.   Chessell IP, Hatcher JP, Bountra C, Michel AD, Hughes JP, Green P *et al.* Disruption of the P2X7 purinoceptor gene abolishes chronic inflammatory and neuropathic pain. *Pain* 2005; **114:** 386-396.

31.   Nicke A, Kuan YH, Masin M, Rettinger J, Marquez-Klaka B, Bender O *et al.* A functional P2X7 splice variant with an alternative transmembrane domain 1 escapes gene inactivation in P2X7 knock-out mice. *J Biol Chem* 2009; **284:** 25813-22.

32.   Schwarz N, Drouot L, Nicke A, Fliegert R, Boyer O, Guse AH *et al.* Alternative splicing of the N-terminal cytosolic and transmembrane domains of P2X7 controls gating of the ion channel by ADP-ribosylation. *PLoS ONE* 2012; **7:** e41269.

33.   Taylor SRJ, Gonzalez-Begne M, Sojka DK, Richardson JC, Sheardown SA, Harrison SM *et al.* Lymphocytes from P2X7-deficient mice exhibit enhanced P2X7 responses. *J Leuk Biol* 2009; **85:** 978-986.

34.   Davies B, Brown PD, East N, Crimmin MJ, Balkwill FR. A synthetic matrix metalloproteinase inhibitor decreases tumor burden and prolongs survival of mice bearing human ovarian carcinoma xenografts. *Cancer Res* 1993; **53:** 2087-91.

35.   Ludwig A, Hundhausen C, Lambert MH, Broadway N, Andrews RC, Bickett DM *et al.* Metalloproteinase inhibitors for the disintegrin-like metalloproteinases ADAM10 and ADAM17 that differentially block constitutive and phorbol ester-inducible shedding of cell surface molecules. *Comb Chem High Throughput Screen* 2005; **8:** 161-71.

36.   Fourie AM, Coles F, Moreno V, Karlsson L. Catalytic activity of ADAM8, ADAM15, and MDC-L (ADAM28) on synthetic peptide substrates and in ectodomain cleavage of CD23. *J Biol Chem* 2003; **278:** 30469-77.

37.   Syberg S, Schwarz P, Petersen S, Steinberg TH, Jensen JE, Teilmann J *et al.* Association between P2X7 receptor polymorphisms and bone status in mice. *J Osteoporos* 2012; **2012:** 637986.

38.   Jackson L, Cady CT, Cambier JC. TLR4-mediated signaling induces MMP9-

        dependent cleavage of B cell surface CD23. *J Immunol* 2009; **183:** 2585-92.

39.   Hoshino K, Takeuchi O, Kawai T, Sanjo H, Ogawa T, Takeda Y *et al.* Cutting

        edge: Toll-like receptor 4 (TLR4)-deficient mice are hyporesponsive to

        lipopolysaccharide: evidence for TLR4 as the Lps gene product. *J Immunol*

        1999; **162:** 3749-52.

40.   Lester S, Stokes L, Skarratt KK, Gu BJ, Sivils KL, Lessard CJ *et al.* Epistasis

        with HLA DR3 implicates the P2X7 receptor in the pathogenesis of primary

        Sjogren's syndrome. *Arthritis Res Ther* 2013; **15:** R71.

41.   Woods LT, Camden JM, Batek JM, Petris MJ, Erb L, Weisman GA. P2X7

        receptor activation induces inflammatory responses in salivary gland

        epithelium. *Am J Physiol Cell Physiol* 2012; **303:** C790-801.

42.   Baldini C, Rossi C, Ferro F, Santini E, Seccia V, Donati V *et al.* The P2X7

        receptor-inflammasome complex has a role in modulating the inflammatory

        response in primary Sjogren's syndrome. *J Intern Med* 2013; **274:** 480-9.

43.   Huissoon AP, Emery P, Bacon PA, Gordon J, Salmon M. Increased

        expression of CD23 in rheumatoid synovitis. *Scand J Rheumatol* 2000; **29:**

        154-9.

44.   Ribbens C, Bonnet V, Kaiser MJ, Andre B, Kaye O, Franchimont N *et al.*
        Increased synovial fluid levels of soluble CD23 are associated with an erosive
        status in rheumatoid arthritis (RA). *Clin Exp Immunol* 2000; **120:** 194-9.

45.   Bansal A, Roberts T, Hay EM, Kay R, Pumphrey RS, Wilson PB. Soluble
        CD23 levels are elevated in the serum of patients with primary Sjogren's
        syndrome and systemic lupus erythematosus. *Clin Exp Immunol* 1992; **89:**
        452-5.

46.   Schellekens GA, de Jong BA, van den Hoogen FH, van de Putte LB, van
        Venrooij WJ. Citrulline is an essential constituent of antigenic determinants
        recognized by rheumatoid arthritis-specific autoantibodies. *J Clin Invest* 1998;
        101: 273-81.

47.   Bendaoud B, Pennec YL, Lelong A, Le Noac'h JF, Magadur G, Jouquan J *et
        al.* IgA-containing immune complexes in the circulation of patients with
        primary Sjogren's syndrome. *J Autoimmun* 1991; **4:** 177-84.

48.   Philpott NJ, Turner AJC, Westby M, Marsh JCW, Gordon-Smith EC,
        Dalgleish AG *et al.* The use of 7-amino actinomycin D identifying apoptosis:
        Simplicity of use and broad spectrum of application compared with other
        techniques. *Blood* 1996; **87:** 2244-2251.

49.   Gu BJ, Zhang WY, Worthington RA, Sluyter R, Dao-Ung P, Petrou S *et al.* A

Glu-496 to Ala polymorphism leads to loss of function of the human P2X$_7$

receptor. *J Biol Chem* 2001; **276:** 11135-11142.

50.   Tsukimoto M, Maehata M, Harada H, Ikari A, Takagi K, Degawa M. P2X7

receptor-dependent cell death is modulated during murine T cell maturation

and mediated by dual signaling pathways. *J Immunol* 2006; **177:** 2842-50.

51.   Schmid I, Uittenbogaart CH, Giorgi JV. A gentle fixation and

permeabilization method for combined cell surface and intracellular staining

with improved precision in DNA quantification. *Cytometry* 1991; **12:** 279-85.

52.   Gadeock S, Pupovac A, Sluyter V, Spildrejorde M, Sluyter R. P2X7 receptor

activation mediates organic cation uptake into human myeloid leukaemic KG-

1 cells. *Purinergic Signal* 2012; **8:** 669-76.

53.   Spildrejorde M, Bartlett R, Stokes L, Jalilian I, Peranec M, Sluyter V *et al.* A

R270C polymorphism leads to loss of function of the canine P2X7 receptor.

Physiol Genomics 2014; doi: 10.1152/physiolgenomics.00195.2013.

.

Figure 1 P2X7 activation induces CD23 shedding from human B cells. (a, b) PBMCs in NaCl medium were incubated for up to 30 min at 37°C in the absence or presence of 1 mM ATP as indicated. (c) Cells in NaCl medium were incubated in the absence (basal) or presence of 1 mM ATP, 0.3 mM BzATP, 1 mM ADP or 1 mM UTP at 37°C for 6 min. (d) PBMCs in NaCl medium were preincubated at 37°C for 15 min in the absence or presence of 100 nM AZ10606120 (AZ) and then in the absence (basal) or presence of 1 mM ATP for 6 min at 37°C. (a-d) Incubations were stopped by addition of $MgCl_2$ medium and centrifugation. PBMCs were labelled with APC-conjugated anti-CD19, PE-conjugated anti-CD23 or isotype control mAb and 7AAD. The mean fluorescence intensity of cell-surface CD23 expression on $CD19^+7AAD^-$ B cells was determined by flow cytometry. (e) PBMCs in NaCl medium were incubated in the absence (basal) or presence of 1 mM ATP at 37°C for 20 min, incubations were stopped by centrifugation and the amount of soluble CD23 in cell-free supernatants determined by ELISA. (a) Histograms (from one representative individual) show CD23 expression on (black or grey fill) or isotype control mAb binding (black line) to $CD19^+7AAD^-$ PBMCs incubated in the absence (black fill or black line) or presence (grey fill) of 1 mM ATP for 30 min; isotype control mAb binding to $CD19^+7AAD^-$ PBMCs incubated in the presence of ATP was similar to that of cells incubated in the absence of ATP (not shown). (b-e) Results are mean ± SD (3 individuals); $^*P < 0.05$ and $^{**}P < 0.01$ compared to basal, and $^\dagger P < 0.05$ compared to ATP alone.

Figure 2 C57BL/6 and DBA/1 murine B cells express functional P2X7. (a, b) Splenic cells in NaCl medium were pre-incubated in the absence or presence of 10 μM AZ10606120 at 37°C for 15 min. Cells were then incubated with 1 μM YO-PRO-1^{2+}

in the absence (basal) or presence of 1 mM ATP at 37°C for 15 min. Incubations were stopped by the addition of MgCl$_2$ medium and centrifugation. Cells were labelled with APC-conjugated anti-CD19 and 7AAD, and the mean fluorescence intensity of YO-PRO-1^{2+} uptake on CD19$^+$7AAD$^-$ B cells was determined by flow cytometry. Results are mean ± SD ((a) 3 mice, or (b) duplicate values from 2 mice); $^{**}P < 0.01$ compared to control, and $^{††}P < 0.01$ compared to ATP alone.

Figure 3 P2X7 activation induces CD23 shedding from B cells from C57BL/6 and DBA/1 mice. (a-c) Splenic cells in NaCl medium were incubated for up to 30 min at 37°C in the absence or presence of 1 mM ATP as indicated. (d, e) Splenic cells in NaCl medium were incubated in the absence (basal) or presence of 1 mM ATP, 0.3 mM BzATP, 1 mM ADP or 1 mM UTP at 37°C for 7 min. (f, g) Splenic cells in NaCl medium were preincubated at 37°C for 15 min in the absence or presence of 10 μM AZ10606120 (AZ) and then in the absence (basal) or presence of 1 mM ATP for 7 min at 37°C. (h) Splenic cells from wild-type (WT) or P2X7 knockout (KO) C57BL/6 mice in NaCl medium were incubated in the absence (basal) or presence of 1 mM ATP for 20 min at 37°C. (a-h) Incubations were stopped by addition of MgCl$_2$ medium and centrifugation. Cells were labelled with APC-conjugated anti-CD19, FITC-conjugated anti-CD23, or isotype control mAb and 7AAD. (a, b) Histograms (from one representative (a) C57BL/6 or (b) DBA/1 mouse) show CD23 expression on (black or grey fill) or isotype control mAb binding (black line) to CD19$^+$7AAD$^-$ PBMCs incubated in the absence (black fill or black line) or presence (grey fill) of 1 mM ATP for 30 min; isotype control mAb binding to CD19$^+$7AAD$^-$ splenic cells incubated in the presence of ATP was similar to that of cells incubated in the absence
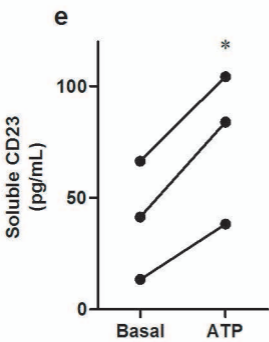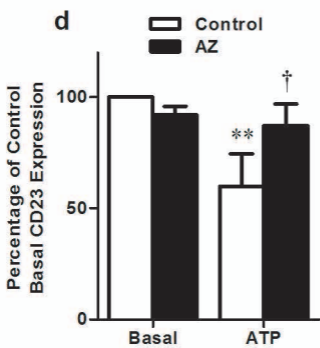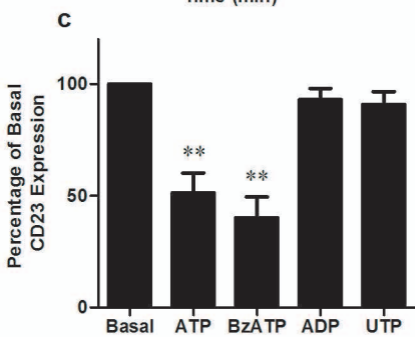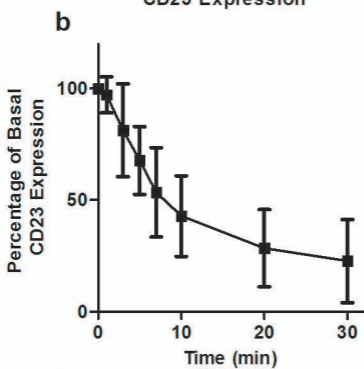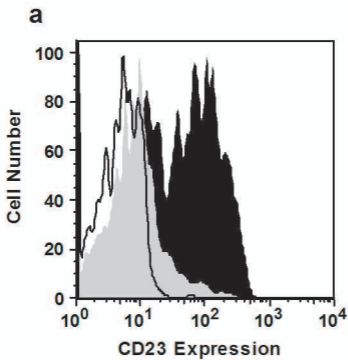
of ATP (not shown). (c-h) The mean fluorescence intensity of CD23 expression on CD19$^+$7AAD$^-$ B cells was determined by flow cytometry. Results are mean ± SD ((c, f) triplicate values from 1 mouse or (d, e, g, h) 3 mice); $^*P < 0.05$ and $^{**}P < 0.01$ compared to control, and $^{††}P < 0.01$ compared to ATP alone.
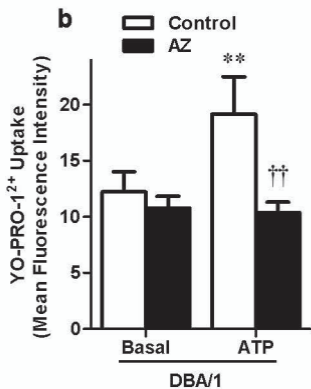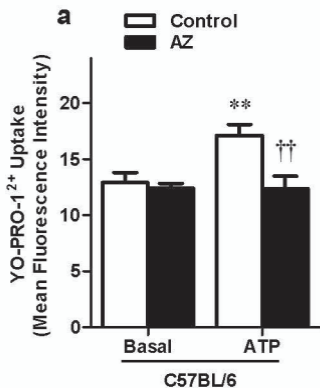
Figure 4 P2X7 activation induces CD23 shedding from B cells from C57BL/6 mice. (a, b) Splenic cells from wild-type (WT) or (b) P2X7 knockout (KO) C57BL/6 mice in NaCl medium were incubated for 20 min at 37°C in the absence (basal) or presence of 1 mM ATP. (a) Incubations were stopped by addition of MgCl$_2$ medium and centrifugation. Cells were labelled with APC-conjugated anti-CD19 mAb and 7AAD, and fixed with paraformaldehyde in PBS. Fixed cells were then labelled with FITC-conjugated anti-CD23 or isotype control mAb in the absence (fixed, F) or presence (fixed and permeabilised, F & P) of Tween-20 in PBS. The mean fluorescence intensity of CD23 expression in CD19$^+$7AAD$^-$ B cells was determined by flow cytometry. (b) Incubations were stopped by centrifugation and the amount of soluble CD23 in cell-free supernatants determined by ELISA. Results are mean ± SD ((a) 3 or (b) 4 mice); $^{**}P < 0.01$ compared to control, and $^{††}P < 0.01$ compared to ATP.
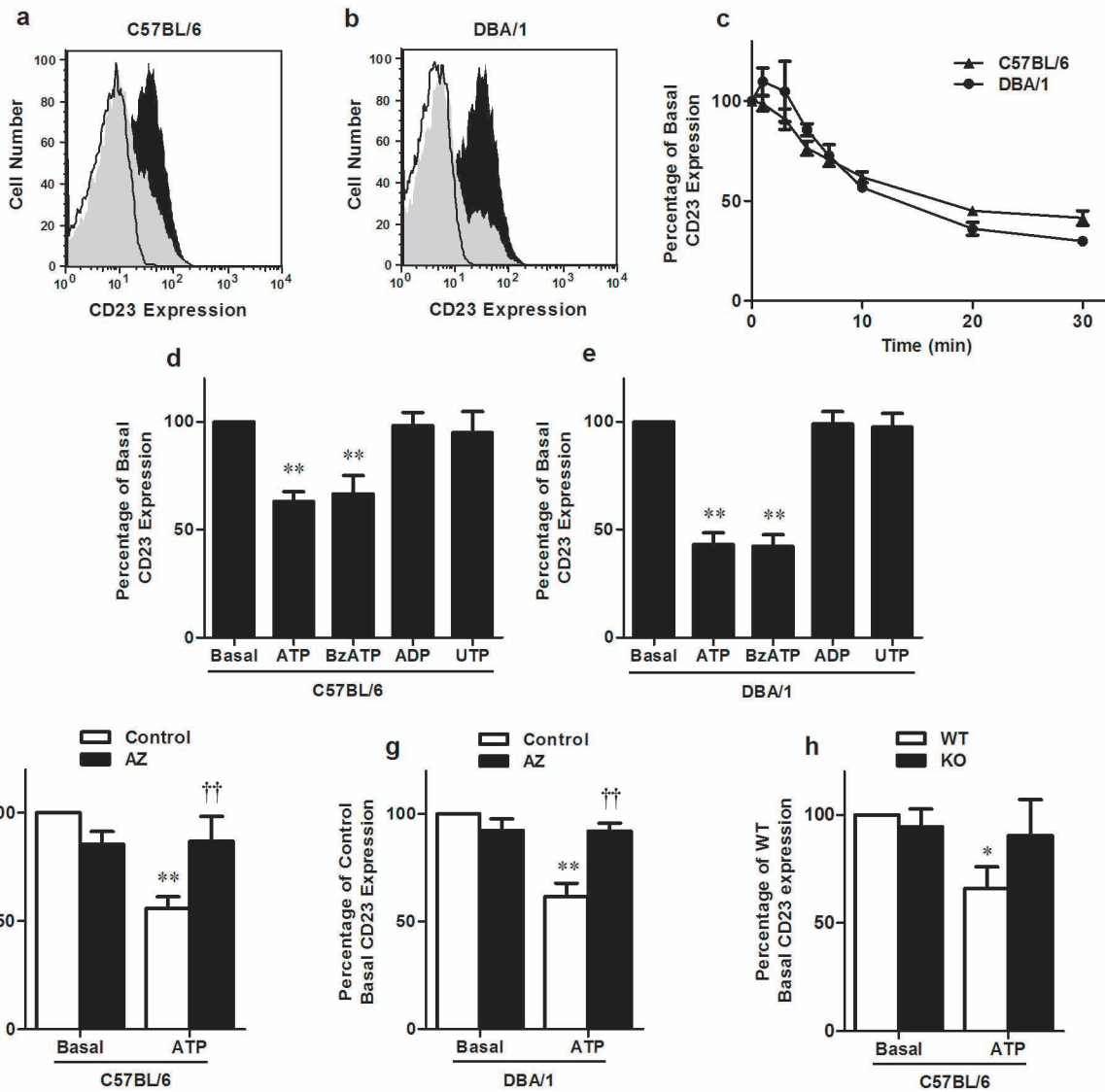
Figure 5 Splenic cells from P2X7 knockout mice do not express full-length, functional P2X7. (a) Relative P2X7 expression in the spleens of wild-type (WT) and P2X7 knockout (KO) C57BL/6 mice was measured by quantitative real time-PCR using primers to exons 1 and 2 of the *P2RX7* gene. (b) Whole lysates of WT and P2X7 KO splenic cells, and RAW 264.7 macrophages (RAW) were examined by immunoblotting using an antibody agonist the extracellular epitope of P2X7. (c)
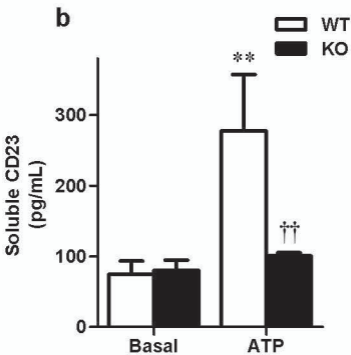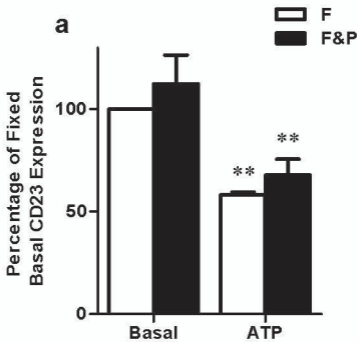
Splenic cells, from WT and P2X7 KO mice, in NaCl medium were incubated with 1 μM YO-PRO-1^{2+} in the absence or presence of 1 mM ATP at 37°C for 15 min. Incubations were stopped by the addition of MgCl$_2$ medium and centrifugation. Cells were labelled with PerCP/Cy5.5-conjugated anti-CD3 mAb and APC-conjugated anti-CD19 mAb, and the mean fluorescence intensity of YO-PRO-1^{2+} uptake into CD3$^-$CD19$^+$ B cells and CD3$^+$CD19$^-$ T cells was determined by flow cytometry. Results are (a, c) mean ± SD (3 mice; points represent individual mice) or (b) one representative of 2 experiments.
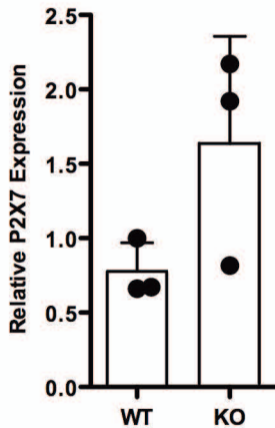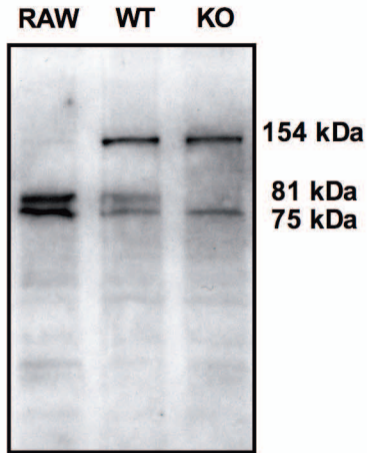
Figure 6 Metalloproteases mediate P2X7-induced shedding from human and murine B cells. (a, d) Human peripheral blood mononuclear cells, and (b, e) C57BL/6 or (c, f) DBA/1 murine splenic cells were preincubated in the presence of (a-f) DMSO, (a-c) 1 μM BB-94 (BB) or (d-f) 3 μM GI254023X (GI), and (a-f) then in the absence (basal) or presence of 1 mM ATP at 37°C for 7 min. Incubations were stopped by addition of MgCl$_2$ medium and centrifugation. B cells were labelled with APC-conjugated anti-CD19 mAb, PE- or FITC-conjugated anti-CD23, or isotype control mAb and 7AAD. The mean fluorescence intensity of cell-surface CD23 expression on CD19$^+$7AAD$^-$ B cells was determined by flow cytometry. Results are mean ± SD ((a) 4 or (d) 3 individuals, or (b, c, e, f) 3 mice); $^*P < 0.05$ and $^{**}P < 0.01$ compared to control, and $^{††}P < 0.01$ compared to ATP alone.

a

b

c

d

e

a

Control
AZ

YO-PRO-1^{2+} Uptake
(Mean Fluorescence Intensity)

**

††

Basal   ATP

C57BL/6

b

Control
AZ

YO-PRO-1^{2+} Uptake
(Mean Fluorescence Intensity)

**

††

Basal   ATP

DBA/1

a